J Ind Microbiol Biotechnol (2008) 35:525–531
DOI 10.1007/s10295-008-0311-3

ORIGINAL PAPER

Expressions of mass transfer coefficients of bubbles and free surface of culture tanks using the k–ε turbulence model

Ken Amano · Ryoichi Haga · Sei Murakami

Received: 24 January 2007 / Accepted: 19 December 2007 / Published online: 18 March 2008

Abstract For mammalian cell culture, getting a continuous supply of oxygen and extracting carbon dioxide are primary challenges even in the most modern biopharmaceutical manufacturing plants, due to the low oxygen solubility and excessive carbon dioxide accumulation. In addition, various independent flow and mass transfer characteristics in the culture tanks vessel make scale-up extremely difficult. One method for overcoming these and providing rational optimization is solving the fluid and mass transport equations by numerical simulation. To develop a simulation program, it is decisively important to know mass transfer coefficients of gaseous species in the culture tank. In this study, oxygen mass transfer coefficients are measured using a beaker with a sparger and impellers. In order to investigate the formulation of the mass transfer coefficients, the turbulent flow statistics is calculated by a CFD code for all cases, and the expressions of the mass transfer coefficients are established as functions of the statistics. Until now, the expression by Kawase is known in this field. This expression becomes a function only of energy dissipation rate ε. It does not coincide with the conventional experimental fact that mass transfer coefficient is proportional power 0.5 of impeller rotation speed. The new mass transfer coefficient is dependent on both of energy dissipation rate ε and turbulent flow energy k. It satisfies the relation of power of 0.5 of impeller rotation speed.

K. Amano (✉) · R. Haga
Power & Industrial Systems R&D Laboratory, Hitachi, Ltd.,
7-2-1 Omika-cho, Hitachi, Ibaragi 319-1221, Japan
e-mail: ken.amano.yv@hitachi.com

S. Murakami
Industrial Systems Div., Hitachi Plant Technology, Ltd.,
2-9-7 Ikenohata, Taito-ku, Tokyo 110-0008, Japan

Keywords Mass transfer capacity coefficient · Cell culture tank · Agitation · Turbulent energy · Energy dissipation rate

Introduction

In mammalian cell culture, it is important to uniformly supply oxygen and rapidly remove metabolite carbon dioxide. But, it is difficult to make the culture medium in a large culture tank homogeneous, and carbon dioxide is easily accumulated. Even if a model experiment with a small culture tank is done, the phenomena are not similar between small and large tanks, since the flow is usually two-phase bubbly flow and it contains metabolic reaction products.

One method which overcomes this difficulty is to solve the equations of the flow and related transport equations by numerical simulation. Nowadays, several computational fluid dynamics (CFD) codes are available which solve the two-phase turbulent flow. When these codes are utilized to design culture tanks, the mass transfer coefficient and some metabolic reactions must be considered in the CFD codes.

There are two common ways to provide oxygen, one is bubbles from a sparger and the other is diffusion from the liquid surface. But, the mathematical expressions of the mass transfer coefficients at the two kinds of interfaces may be different, because the flow boundary conditions at the interfaces are apparently different. Therefore, both mass transfer coefficient expressions should be obtained separately.

Some investigations [1, 2] have given the mass transfer coefficient for bubble columns or bioreactors experimentally. The coefficient has commonly been expressed using bubble diameter, gravity acceleration, liquid density, surface tension, etc., with the diameter of the bubble column

being especially important. However, these empirical formulae may be dependent on the shape of the column, and they may not have generality.

It can be conceptually considered that the mass transfer coefficient is a function of turbulent flow statistics as well as physical properties of the liquid and gases. Until now, the expression by [3] is known in this field. Turbulent energy k and energy dissipation rate ε are well defined turbulent flow statistics in the turbulent flow theory. Launder et al. [4] developed a model of transport equations of k and ε for numerical simulation. Today, the k–ε model is considered an outstanding turbulence model and is incorporated into many CFD codes. Strictly speaking, the numerical values of the k and ε may depend on the model equations and the discretion techniques of the equations, that is, they may depend on the CFD code itself. However, as numerical simulation is a powerful design tool, it is worthwhile finding expressions of the mass transfer coefficient as a function of k and ε by the k–ε model.

In this study, we measure oxygen mass transfer coefficients at two kinds of interfaces using a beaker with a sparger and an impeller. The distributions of the turbulent flow statistics in the beaker are also calculated by a CFD code; we choose R-FLOW[5]. R-FLOW can solve a set of multi-phase flow equations and the k-ε model. It can also handle the motion of the impeller by the "sliding mesh" or "overset mesh" technique.

Using these results, we establish the expressions of the mass transfer coefficients as functions of turbulent flow statistics k and ε.

Materials and methods

$K_L a$ measurement

In the following description, the mass transfer capacity coefficient is designated as K_L a and the mass transfer coefficient is designated as K_L. The K_L a is the product of K_L and the specific surface area a.

A beaker (15 cm diameter) containing Phosphate Buffer Saline is used for the measurement of K_L a . Two liquid volumes are tested, 2.65 and 5.3 L. The level height of the 2.65 L beaker is 15 cm, and the twice for the 5.3 L beaker. The beaker arrangement is shown in Fig. 1. Two enzyme electrode DO sensors are inserted from the top. Two types of impellers are tested, a flat paddle and a marine screw . Both wing diameters are 10 cm. The sparger material is porous sintered compact with average pore size of 100 microns. The bubble diameter is dependent on the sparger pore size. Hardly any division and coalescence of the bubbles occur in the flow. The bubble diameter is measured from photographs of bubbles in the flow taken using a high speed camera.

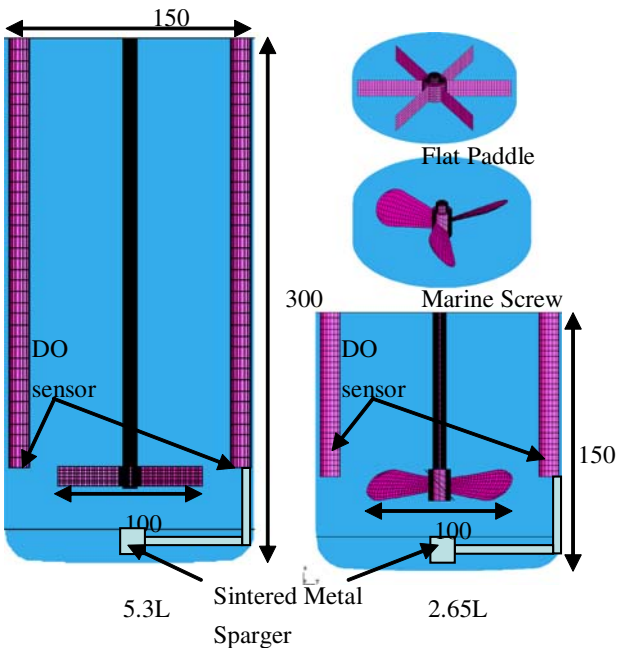

Fig. 1 Configuration of the beaker for K_L a measurement

Figure 2 reproduces an example photograph of the bubbles, and Fig. 3 shows the distribution of the bubble diameter as particle numbers in that photo. In the CFD code, the bubble diameter is handled as a unique constant value, and the bubble size distribution can not be considered. We obtain the bubble diameter as 1.2 mm from Fig. 3. Measuring the terminal velocity of the bubbles is difficult, so we decide it according to a mathematical model.

The mass transfer capacity coefficient K_L a is measured by the gassing out method. The liquid is deaerated by supplying nitrogen from the sparger until the dissolved oxygen decreases at 1 mg/L or less. After the supply of

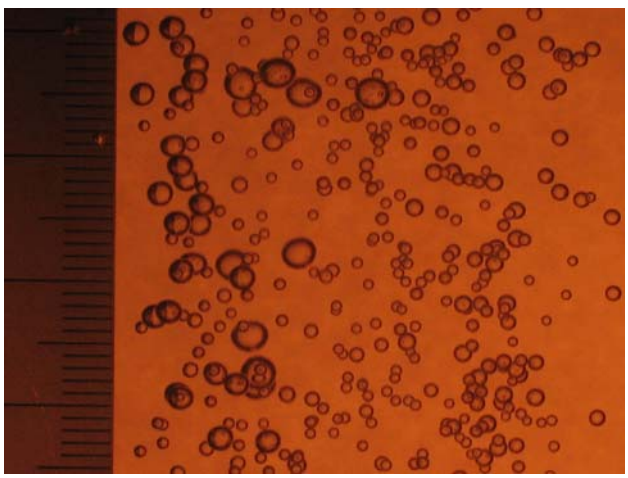

Fig. 2 Photograph of bubbles from the sparger

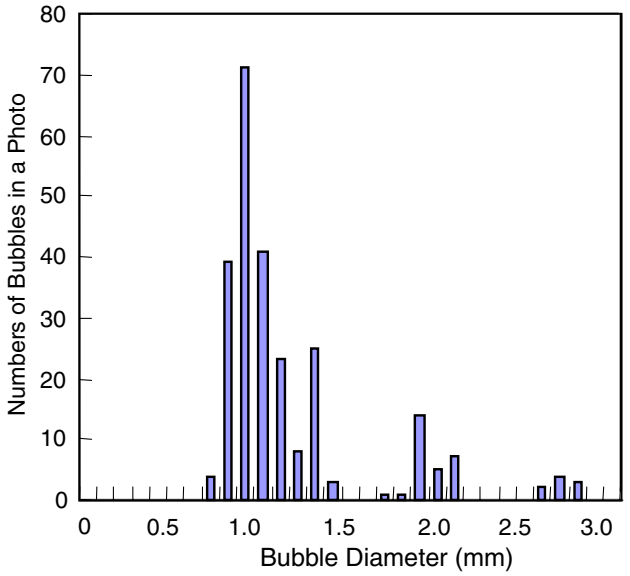

Fig. 3 Distribution of bubble diameter

nitrogen from the sparger is stopped, air is blown in at a constant flow rate of 120 mL/min by stirring with a constant impeller rotation speed. The liquid surface is open to the air. The time changes of the dissolved oxygen are measured at 2-min intervals until the concentration is almost stabilized at a constant value, and seems to have reached a saturation state. In addition to the above measurements, the rise in the dissolved oxygen is also measured considering only diffusion penetration from the liquid surface without oxygen supply from the sparger for all cases.

When oxygen is supplied from the sparger, the time change of the dissolved oxygen is given as

$$\frac{\mathrm{dDO}}{\mathrm{d}t} = \mathrm{K_{LB}}a_{\mathrm{B}}(\mathrm{DO_B^{eq}} - \mathrm{DO}) + K_{\mathrm{LS}}a_{\mathrm{S}}\left(\mathrm{DO_S^{eq}} - \mathrm{DO}\right), \quad (1)$$

where, K_{LB} and K_{LS} are mass transfer coefficients of bubbles and liquid surface, a_{B} and a_{S} are the specific surface areas, and $\mathrm{DO_B^{eq}}$, and $\mathrm{DO_S^{eq}}$ are the dissolved oxygen concentrations which balance with the partial oxygen pressure, respectively. The specific surface area a_{B} is bubble surface area per unit volume, and the specific surface area a_{S} is defined as liquid surface area/liquid volume.

From Eq. (1), the time change of dissolved oxygen is given as

$$\mathrm{DO}(t) = \mathrm{DO}(1 - \exp(-\lambda t)), \quad (2)$$

where,

$$\lambda = \mathrm{K_{LB}}a_{\mathrm{B}} + \mathrm{K_{LS}}a_{\mathrm{S}}$$

$$\overline{\mathrm{DO}} = \left(\mathrm{K_{LB}a_B DO_B^{eq}} + \mathrm{K_{LS}a_S DO_S^{eq}}\right)/\lambda.$$

Without the sparger gas supply, it is

$$\mathrm{DO}(t) = \mathrm{DO}(1 - \exp(-\lambda t)), \quad (3)$$

where, $\lambda = K_{\mathrm{LS}}\, a_{\mathrm{S}}$ and $\overline{\mathrm{DO}} = \left(K_{\mathrm{LS}}a_{\mathrm{S}}\mathrm{DO_S^{eq}}\right)/\lambda$.

By fitting the measured data to Eqs. (2) and (3), $K_{\mathrm{L}}\, a_{\mathrm{B}}$ and $K_{\mathrm{L}}\, a_{\mathrm{S}}$ are determined separately. Example measurements obtained by the gassing out method are shown in Fig. 4.

For all measurement cases, the steady turbulent flow statistics k and ε are calculated by the CFD code. The drift flux model is used as the analytical model of two-phase flow. The model means that the acceleration of the bubbles is 0. The motion equation of liquid flow is solved, but that of bubbles is not solved by the drift flux model. The bubble velocity U_{B} is always obtained as a summation of the liquid flow velocity U_{F} and the bubble terminal velocity U_{D}.

$$U_{\mathrm{B}} = U_{\mathrm{F}} + U_{\mathrm{D}} \quad (4)$$

The terminal velocity U_{D} is deduced from the balance of drag force and buoyancy of a bubble. The motion equation of a bubble is

$$\begin{aligned}\frac{\pi}{6}D_B^3\rho_{\mathrm{B}}\frac{\mathrm{d}U_{\mathrm{B}}}{\mathrm{d}t} &= \frac{\pi}{8}D_{\mathrm{B}}^2 C_{\mathrm{D}}\rho_{\mathrm{F}}|U_{\mathrm{F}} - U_{\mathrm{B}}|(U_{\mathrm{F}} - U_{\mathrm{B}}) \\ &\quad + \frac{\pi}{6}D_{\mathrm{B}}^3(\rho_{\mathrm{F}} - \rho_{\mathrm{B}})g \\ &= 0\end{aligned} \quad (5)$$

where,

$$\begin{aligned}C_{\mathrm{D}} &= 24 \times \left(1 + 0.15 * Re^{0.678}\right)/Re \quad (Re < 1,000) \\ &= 0.44 \quad (Re > 1,000)\end{aligned}$$

and

$$Re = \frac{U_{\mathrm{F}}\mathrm{D}_B}{v}.$$

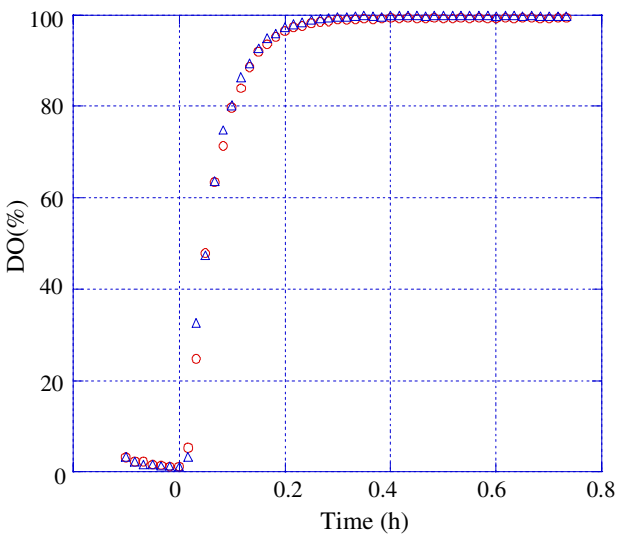

Fig. 4 Measured data obtained by the gassing out method

From Eq. (5), the terminal velocity is solved as

$$U_{\mathrm{D}} = \sqrt{\frac{4}{3}\frac{D_{\mathrm{B}}}{C_{\mathrm{D}}}\frac{(\rho_{\mathrm{F}} - \rho_{\mathrm{B}})g}{\rho_F}}. \quad (6)$$

For a bubble of 1.2 mm diameter, the terminal velocity is about 11 cm/s.

The k–ε model is described in the following equations.

The definitions of the turbulent energy k and its dissipation rate $\varepsilon$are defined as

$u_i = \overline{u_i} + u_i'$

$\overline{u_i}$: average velocity u_i' : fluctuation from the average

$$k = \frac{1}{2}\sum_{i=1}^{3}\overline{u_i' u_i'}$$

$$\varepsilon = \frac{v}{2}\sum_{i,j=1}^{3}\overline{\left(\frac{\partial u_i'}{\partial x_j} + \frac{\partial u_j'}{\partial x_i}\right)^2}.$$

The k–ε model solves two transport equations as follows

$$\frac{\partial k}{\partial t} + (\bar{\mathbf{u}}\cdot\nabla)k = \nabla\cdot\left(\frac{v_t}{\sigma_k}\nabla k\right) + P_{\mathrm{K}} - \varepsilon, \quad (7)$$

where

$$P_{\mathrm{K}} = \frac{v_t}{2}\sum_{i,j=1}^{3}\left(\frac{\partial \bar{u}_i}{\partial x_j} + \frac{\partial \bar{u}_j}{\partial x_i}\right)^2 v_t = c_\mu\frac{k^2}{\varepsilon},$$

and

$$\frac{\partial \varepsilon}{\partial t} + (\bar{\mathbf{u}}\cdot\nabla)\varepsilon = \nabla\cdot\left(\frac{v_t}{\sigma_\varepsilon}\nabla\varepsilon\right) + c_1\frac{\varepsilon}{k}P_{\mathrm{K}} - c_2\frac{\varepsilon^2}{k}, \quad (8)$$

$C_1 = 1.44,\ C_2 = 1.92,\ C_\mu = 0.09.$

Example flow simulation results for a beaker are shown in Fig. 5. They include the distributions of the flow velocity, the turbulent energy, the energy dissipation rate, and the gas holdup. From the gas holdup α, the specific surface area can be estimated as $a_{\mathrm{B}} = \frac{6\alpha}{D_{\mathrm{B}}}$.

Results

Measured $K_{\mathrm{L}}\ a$ and turbulent flow statistics obtained by numerical simulations are shown in Tables 1 and 2. The marine screw cases are operated with a higher rotation speed than those of the flat paddle, because power consumption of the marine screw is smaller than that of the flat paddle and intensity of turbulence is also smaller. Table 1 lists the measured mass transfer capacity coefficient $K_{\mathrm{LB}}\ a_{\mathrm{B}}$ and mean values of the turbulent flow statistic in the beaker. Tables 2 lists the measured mass transfer coefficient K_{LS} and mean values of the turbulent flow statistics at the horizontal surface 5 mm deep from the top level. Intensity of turbulence weakens at the surface, because the surface is far from the impeller for both beakers. The weakening is more significant for the 5.3 L beaker.

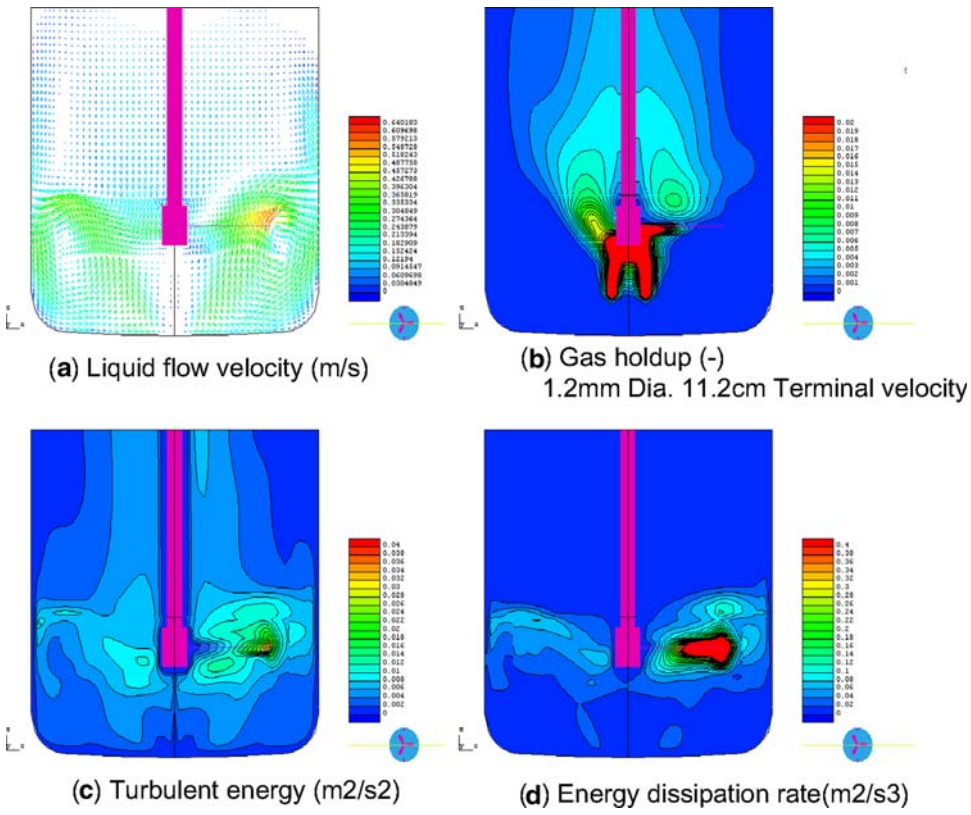

Fig. 5 Example numerical flow simulation results

Table 1 Calculated turbulent flow statistics and measured $K_L a$ of bubbles

		k	ε	$(v\varepsilon)^{0.25}$	$(k^2/v\ \varepsilon)^{Gas}$	α^{Holdup}	$K_{LB}a_B$ (s^{-1})
Flat paddle							
2.65 L	80 rpm	0.00495	0.01050	0.00941	2,711	0.00179	0.00458
	120 rpm	0.01230	0.03930	0.01310	4,394	0.00161	0.00557
	160 rpm	0.02200	0.09360	0.01620	5,894	0.00139	0.00681
5.30 L	80 rpm	0.00199	0.00429	0.00630	1,425	0.00168	0.00381
	120 rpm	0.00492	0.01590	0.00880	2,343	0.00146	0.00450
	160 rpm	0.00878	0.03770	0.01090	3,137	0.00134	0.00541
Marine screw							
2.65 L	120 rpm	0.00180	0.00970	0.00789	751	0.00137	0.00412
	160 rpm	0.00375	0.02430	0.01020	1,205	0.00139	0.00541
	200 rpm	0.00616	0.04830	0.01210	1,565	0.00142	0.00612
5.30 L	120 rpm	0.00046	0.00319	0.00459	332	0.00113	0.00338
	160 rpm	0.00067	0.00713	0.00518	263	0.00126	0.00369
	200 rpm	0.00115	0.01410	0.00622	406	0.00134	0.00458

Table 2 Calculated turbulent flow statistics and measured K_L at surface

		k_S	ε_S	$(v\varepsilon)_S^{0.25}$	$(k^2/v\varepsilon)_S$	K_{LS} (ms)
Flat paddle						
2.65 L	80 rpm	0.00346	0.00439	0.00941	2,882	0.0000479
	120 rpm	0.00937	0.02010	0.01310	4,723	0.0000767
	160 rpm	0.01680	0.04840	0.01620	6,315	0.0000950
5.30 L	80 rpm	0.00028	0.00010	0.00630	828	0.0000233
	120 rpm	0.00056	0.00028	0.00880	1,219	0.0000316
	160 rpm	0.00098	0.00068	0.01090	1,549	0.0000358
Marine screw						
2.65 L	120 rpm	0.00077	0.00082	0.00789	745	0.0000425
	160 rpm	0.00189	0.00313	0.01020	1,205	0.0000608
	200 rpm	0.00310	0.00681	0.01210	1,501	0.0000633
5.30 L	120 rpm	0.00016	0.00017	0.00282	372	0.0000216
	160 rpm	0.00026	0.00049	0.00345	434	0.0000292
	200 rpm	0.00052	0.00082	0.00443	671	0.0000350

K_L has the dimension of velocity (m/s). By using moving viscosity v, turbulent energy k, and energy dissipation rate, $(\varepsilon v)^{0.25}$ and $K^{0.5}$ can be constructed as quantities with dimension of velocity. Here, K_L is expressed using $(\varepsilon v)^{0.25}$ and a dimensionless quantity $k^2/\varepsilon v$ and dimensionless number (D/v), where D is diffusion coefficient.

So, K_L can be assumed in a general form as,

$$K_L = F\left(D/v, k^2/v\varepsilon\right)(v\varepsilon)^{0.25}. \tag{9}$$

Kawase et al. [3] proposed an expression for K_L

$$K_L = 0.301\left(\frac{D}{v}\right)^{0.5}(v\varepsilon)^{0.25}. \tag{10}$$

D/v is the ratio of diffusion flux and momentum flux.

Equation (10) does not include the turbulent energy k. In this study, we assume the following expression and then, optimum value of the power multiplier Y is searched for.

$$K_L = A\left(\frac{D}{v}\right)^{0.5}\left(\frac{k^2}{v\varepsilon}\right)^{Y}(v\varepsilon)^{0.25} \tag{11}$$

Using the 12 data in Table 1, we define the proportion factor $A_i(Y)$ as

$$A_i(Y) = (K_{LB}a_B)_i \Big/ \left[\left(\frac{D}{v}\right)^{0.5}\left(\frac{k^2}{v\varepsilon}\right)_i^{Y}(v\varepsilon)_i^{0.25}\frac{6\alpha_i}{D_B}\right] \tag{12}$$

where, $D = 3.4 \times 10^{-9}$ (m^2/s), $v = 1 \times 10^{-6}$(m^2/s), $D_B = 0.0012$ (m) are adopted.

The average

$$\overline{A(Y)} = \frac{1}{12}\sum_{i=1}^{12} A_i(Y) \tag{13}$$

and the standard deviation

$$\sigma_A(Y) = \sqrt{\frac{1}{12}\sum_{i=1}^{12}\frac{\left(A_i(Y) - \overline{A(Y)}\right)^2}{\overline{A(Y)}^2}} \tag{14}$$

are calculated by changing the power multiplier Y.

Figure 6 graphs the standard deviation of Eq. (14). The value −0.25 of the power multiplier minimizes the standard deviation, and the average proportionality constant is 5.0.

So the expression for K_{LB} is presented as

$$K_{LB} = 5.0\left(\frac{D}{v}\right)^{0.5}\left(\frac{k^2}{v\varepsilon}\right)^{-2.5}(v\varepsilon)^{0.25} = 5.0\sqrt{\frac{\varepsilon D}{k}}. \tag{15}$$

A comparison between experimental and calculated $K_{LB}\ a_B$ values is shown in Fig. 7. The standard deviation σ_A is 12%.

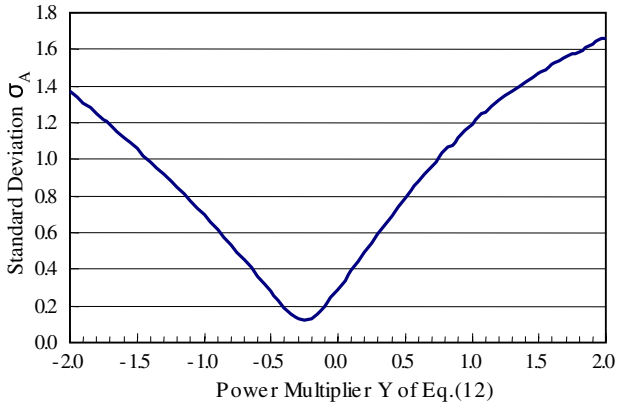

Fig. 6 Standard deviation of Eq. (14) by the measurements of Table 1

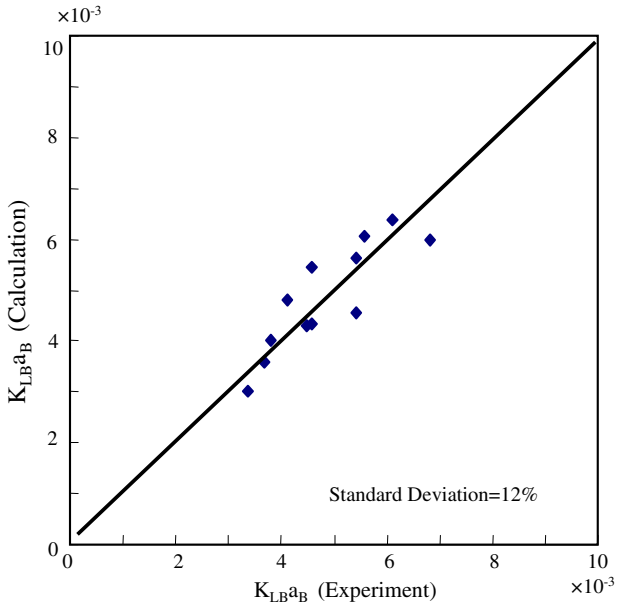

Fig. 7 Comparison between Experiments and Calculations of K_{LB} a_B

In the same manner, using the 12 data of Table 2 we find the expression of K_{LS} at the liquid surface. Here, the proportionality constant is defined as

$$B_i(Y) = (K_{\mathrm{LS}})_i \Big/ \left[\left(\frac{D}{\nu}\right)^{0.5} \left(\frac{k^2}{\nu\varepsilon}\right)_i^{Y} (\nu\varepsilon)_i^{0.25} \right] \tag{16}$$

and the average $B(Y)$ and the standard deviation σ_{B} are calculated.

$$\overline{B(Y)} = \frac{1}{12}\sum_{i=1}^{12} B_i(Y) \tag{17}$$

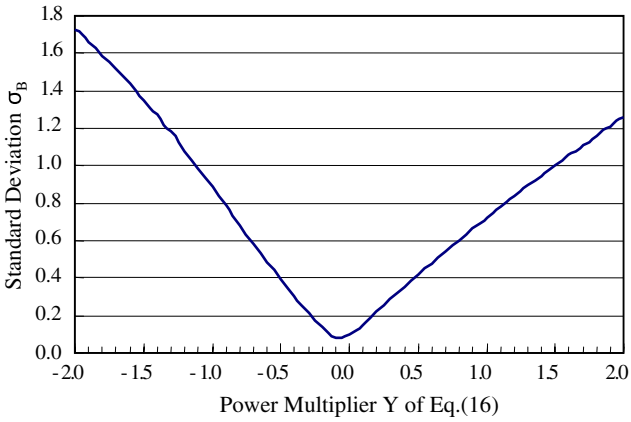

Fig. 8 Standard deviation of Eq. (18) by the measurements of Table 2

$$\sigma_{\mathrm{B}}(Y) = \sqrt{\frac{1}{12}\sum_{i=1}^{12} \frac{\left(B_i(Y) - \overline{B(Y)}\right)^2}{\overline{B(Y)}^2}} \tag{18}$$

Figure 8 shows standard deviation σ_{B}. According to Fig. 8, K_{LS} weakly depends on $(k^2/\varepsilon\nu)$. Here the dependence on $(k^2/\varepsilon\nu)$ is disregarded, and the following expression is presented.

$$K_{\mathrm{LS}} = 0.135\left(\frac{D}{\nu}\right)^{0.5} (\nu\varepsilon)^{0.25} \tag{19}$$

Equation (19) is similar to Eq. (10) of Kawase et al. except for the constant.

Figure 9 compares experimental and calculated K_{LS}.

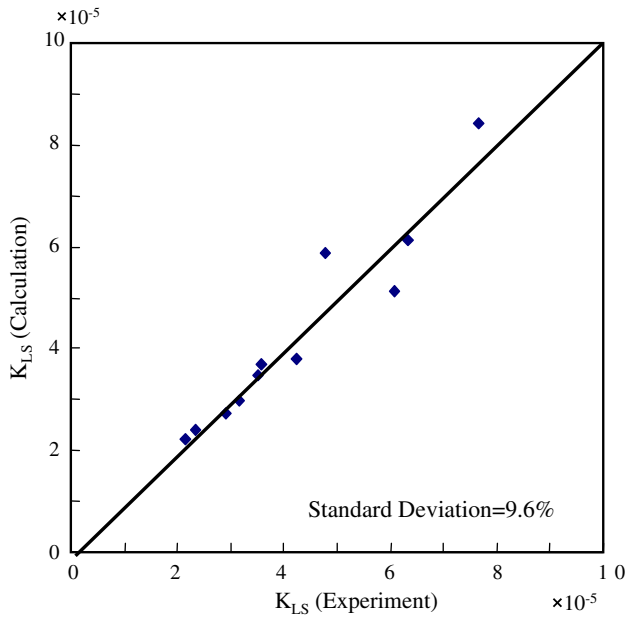

Fig. 9 Comparison between experiments and calculations of K_{LS}

Discussion

Using standard disk turbine blades, Richards [6] experimentally showed that mass transfer coefficient K_L is proportional power 0.5 of the impeller rotation speed. Turbulent flow energy k is proportional to the square of the impeller rotation speed, and the energy dissipation rate ε is proportional to the cube. The equation by Kawase Eq. (10) gives the mass transfer coefficient as a function only of energy dissipation rate. Therefore, the equation by Kawase is proportional power 0.75 of the impeller rotation speed. The new mass transfer coefficient Eq. (15) becomes a function of the turbulent flow energy and the energy dissipation rate, and it is proportional power 0.5 of the impeller rotation speed.

The term of $\left(\varepsilon\nu/k^2\right)^{1/4}$ in Eq. (15) give the ratio of Kolmogorov scale and Taylor's micro scale. The Taylor's micro scale λ is given as

$$\lambda^2 \approx \frac{\overline{u'^2}}{\left(\frac{\partial u'}{\partial x}\right)^2} \approx \frac{k}{(\varepsilon/\nu)}. \tag{20}$$

The Taylor's micro scale gives the representative correlation distance of the flow velocity fluctuation. The Kolmogorov scale η is given as

$$\eta = \left(\frac{\nu^3}{\varepsilon}\right)^{\frac{1}{4}}. \tag{21}$$

The Kolmogorov scale gives the smallest scale of the flow velocity fluctuation. Both ratios become

$$\frac{\eta}{\lambda} = \left(\varepsilon\nu/k^2\right)^{1/4}. \tag{22}$$

Magnussen [7] asserted that the burning rate $\dot{m}$ of the turbulent diffusion flame was given as

$$\dot{m} \propto \left(\frac{\varepsilon\nu}{k^2}\right)^{\frac{1}{4}} \frac{\varepsilon}{k}. \tag{23}$$

The chemical reaction rate of the combustion is so rapid that the burning rate of the diffusion flame is dominated by the hydrodynamic mixing time.

Magnussen asserted that the regions which generate combustion reaction in the turbulent flow field are limited to fine structures, of witch the sizes are as Kolmogorov scale, where micro scale mixing and strong energy dissipation occur. The volume fraction of the fine structures is estimated as $\left(\varepsilon\nu/k^2\right)^{1/4}$ by Magnussen. It may establish the analogy of the similar turbulent mass transport between mass transfer coefficient K_L and burning rate $\dot{m}$.

The discussion of the above can not be applied to the equation of the free liquid level Eq. (19). In the level, the perpendicular flow velocity fluctuation is limited. The flow velocity fluctuation begins to contribute to the mass transport at the region which left the Kolmogorov scale $\left(\nu^3/\varepsilon\right)^{0.25}$ from the level. After all, the mass transfer is dependent on the reciprocal of the thickness of Kolmogorov scale. The mass transfer coefficient of the level may be proportional power 0.25 of ε as Eq. (19).

References

1. Akita K, Yoshida F (1974) Bubble size, interfacial area, and liquid phase mass transfer coefficient in bubble columns. Int Eng Chem Process Des Dev 13:84–91
2. Aunins IG, Groughan MS, Wang DIC (1986) Engineering developments in homogeneous culture of animal cells: oxygenation of reactors and scale up. Biotechnol Bioeng Symp 17:699–723
3. Kawase Y, Halard B, Young MM (1992) Liquid phase mass transfer coefficients in bioreactors. Biotechnol Bioeng 39:1133–1140
4. Launder BE, Spalding DB (1972) Lecture in mathematical models of turbulence. Academic Press, London
5. http://www.rflow.co.jp
6. Richards JW (1961) Studies in aeration and agitation. Prog Ind Microbiol 3:143–172
7. Magnussen BF (1981) On the structure of turbulence and a generalized eddy dissipation concept for chemical reaction in turbulent flow. 19th AIAA aerospace meeting, St. Louis